

Channel Norm-Based User Scheduling Exploiting Channel Asymmetry in Base Station Cooperative Transmission Systems

Shengqian Han, *Student Member, IEEE*, Chenyang Yang, *Senior Member, IEEE*,
and Mats Bengtsson, *Senior Member, IEEE*

Abstract

Base station cooperative transmission, which is also known as coordinated multi-point (CoMP) transmission, is a promising technique to improve spectrum efficiency in future cellular systems. However, they need large signalling overhead to gather the channel information. In this paper, we consider low feedback user scheduling in downlink coherent CoMP systems exploiting their inherent channel asymmetry. Through the analysis of the statistics of the angle between channel vectors and the tightness of a lower bound of the orthogonally projected norm, we show that channel norm provides sufficient information to judge the orthogonality among users in asymmetric channels. Based on this observation, we propose a channel norm-based user scheduler (NUS), a local channel aided NUS (LocalNUS) and a large-scale fading-based user scheduler (LUS). Simulation results show that the LocalNUS performs very close to the existing greedy user scheduler (GUS) and semi-orthogonal user scheduler (SUS) with full channel state information but requiring much lower feedback overhead, the NUS performs close to or even outperforms the GUS and the SUS when limited feedback is considered, and the LUS is robust to time-varying channels.

Index Terms

Coordinated multi-point (CoMP) transmission, user scheduling, low-rate feedback, channel norm.

This work was partly presented at the IEEE GlobCom'09.

S. Han and C. Yang are with the School of Electronics and Information Engineering, Beihang University (BUAA), Beijing, 100191, China (e-mail: sqhan@ee.buaa.edu.cn; cyyang@buaa.edu.cn). M. Bengtsson is with the School of Electrical Engineering, Royal Institute of Technology (KTH), Stockholm, Sweden (e-mail: mats.bengtsson@ee.kth.se).

I. INTRODUCTION

Inter-cell interference (ICI) is one of the major bottlenecks to provide high spectral efficiency in universal frequency reuse cellular networks. Except for various interference mitigation techniques, the concept of cooperative base station (BS) transmission, also known as coordinated multi-point (CoMP) transmission, has attracted much attention recently [1–4].

A typical centralized CoMP system consists of a control unit (CU) and multiple BSs connected to the CU via low-latency backhaul links, where the BSs can be either the distributed antenna heads or the BSs in different cells. As the most promising transmit strategy of CoMP, coherent cooperative transmission using multiuser (MU) precoding can convert ICI into desired signals, with which both the cell-average and the cell-edge throughput can be significantly improved [1,4]. The centralized CoMP system is often regarded as a multiple-input multiple-output (MIMO) system with a "super" BS in literature. This allows existing precoding and user scheduling methods designed for single-cell MU-MIMO systems to be applicable. Nonetheless, there are distinct differences between CoMP MU-MIMO and single-cell MU-MIMO systems, e.g., per-BS power constraints (PBPC) [1,2], asynchronous interference [3] and the composite channels [5].

One fundamental difference between CoMP and single-cell systems lies in the channel characteristic. In single-cell systems the channels from multiple antennas at the BS to each user have the same average energy, whereas in CoMP systems the average channel energy from different BSs to each user differs. Such a feature is inherent in CoMP channels, which is named *channel asymmetry* in this paper. It has large impact on the performance of precoding and scheduling. For instance, the composite channel consisting of both large-scale and small-scale fading experienced by the users in CoMP systems provides a multiuser diversity gain of $\sqrt{2\log K}$ rather than the well-known $\log \log K$, where K is the total number of users [5]. The change of channel feature also provides opportunities to design novel transmission strategies, e.g., [6].

Channel-aware user scheduling is critical in CoMP MU-MIMO systems, where multiple users located in different cells may be selected and served concurrently by several coordinated BSs. When channel state information (CSI) is available at the CU, many scheduling algorithms such as the greedy user scheduler (GUS) [7] and semi-orthogonal user scheduler (SUS) [8] can be applied. However, in the context of CoMP transmission, this leads to large signalling overhead which may counteract the performance gain.

Low feedback user scheduling has been studied extensively for single-cell MU-MIMO systems, see [9–11] and references therein. In [9], the authors point out that both channel direction information (CDI) and channel quality information (CQI) are essential to achieve the full multiuser multiplexing and multiuser diversity gain. In [10], it is shown that the combination of channel norm with long term channel statistics in the form of channel mean and covariance matrix is sufficient for both precoding and scheduling. Considering the fact that most of the feedback overhead comes from the scheduling, a two-phase feedback strategy is proposed in [11], where all users feed back a rough channel information for scheduling in the first stage and only the selected users feed back the refined channel information for precoding in the second stage.

In this paper, we design low feedback schedulers by exploiting the *channel asymmetry* of CoMP systems. We show that such an asymmetric channel exhibits a special spatial correlation. We begin with analyzing the impact of the asymmetry on the orthogonality between users by characterizing the statistic of the angle between their channel vectors. With the derived probability density function (pdf) of the angle between two spatially correlated complex Gaussian vectors, we will show that the orthogonality between users is largely dependent on their locations. Based on the observation, we propose three channel norm-based user schedulers.

For clarification, we call the BS that provides the maximum received power to each user as its local BS, and the other coordinated BSs as non-local BSs. We name the channel from each BS to a user as a sublink channel, and the channel from the local and non-local BS to the user as the local and cross channels, respectively. We will derive a lower bound of the orthogonally projected norm of one user's channel vector onto the subspace spanned by the channel vectors of the other selected users. By maximizing the lower bound, we develop a channel norm-based user scheduler (NUS), with which all users only feed back the instantaneous norms of their sublink channels. To tighten the bound and hence to improve the performance, we proceed to propose a local channel aided NUS (LocalNUS), with which the users feed back both the full local channel and the norms of the cross channels. In [12, 13], another channel norm-based scheduler is proposed, where the users with the largest channel norms are selected. The NUS we proposed can select the users with both high orthogonality and high signal-to-interference-plus-noise ratio (SINR), which is very different from that in [12, 13].

The NUS and the LocalNUS are applicable for the systems with two-phase feedback strategy. In time-varying channels, the resulting scheduling delay may lead to worse orthogonality between

the users scheduled with the outdated channels in the first stage. To address this issue, we propose a large-scale fading gain based user scheduler (LUS), which is based on the fact that the channel norm is dominated by the large-scale fading in CoMP systems. Since the large-scale fading gain varies slowly, the LUS can be quasi-statically performed over a relatively long period.

Limited feedback schemes are often applied for providing CSI to the BS over a capacity-constrained feedback link [14]. The number of feedback bits per user is limited not only by the capacity of its own feedback link [15], but also by the capacity of the overall feedback link shared by all users [16]. Since the proposed schedulers need very low feedback from all users in the first stage and only the selected users feed back the quantized channels for precoding in the second stage, more precise CSI can be provided for precoding than with the GUS and the SUS, which are usually applied in the systems with one-phase feedback strategy. Simulation results demonstrate the performance gain of the proposed schedulers over the GUS and the SUS.

The rest of the paper is organized as follows. The system model is described in Section II. The asymmetric feature of CoMP channels and its impact on the orthogonality between users are investigated in Section III. Three low feedback user schedulers are proposed in Section IV, and their feedback requirement is analyzed in Section V. The performance of the proposed schedulers is compared with existing schedulers using Monte-Carlo simulation in Section VI, and concluding remarks are given in Section VII.

Throughout this paper, boldface upper and lower case letters denote matrices and row vectors, and standard lower case letters denote scalars. The superscripts $(\cdot)^T$ and $(\cdot)^H$ denote the transpose and the conjugate transpose of a vector or a matrix, respectively. $\Re\{\cdot\}$ and $\Im\{\cdot\}$ denote the real and imaginary parts, and $\mathbb{E}\{\cdot\}$ denotes the expectation operator. $\mathbf{A}^{1/2}$ and $|\mathbf{A}|$ respectively denote the Hermitian square-root and the determinant of matrix \mathbf{A} . $\|\mathbf{a}\|$ denotes the Euclidean norm of vector \mathbf{a} , and $\text{diag}\{\mathbf{a}\}$ represents a diagonal matrix with the elements of \mathbf{a} . Finally, \mathbf{I} denotes the identity matrix, and $\mathbf{0}$ denotes the vector of zeros.

II. SYSTEM MODEL

Consider a frequency division duplex (FDD) downlink centralized CoMP systems, as shown in Fig. 1. Through the downlink training, both local and cross channels are available at the user. Then the channel quantization is fed back from each user to its local BS, and all coordinated BSs forward the quantized CSI from local users to the CU through low-latency backhaul links.

Then the CU selects users, computes transmit precoding for the scheduled users, and sends the scheduling results and the precoding weighting vectors to all coordinated BSs for transmission.

Let (M, N_t, K) denote the network layout of the CoMP system consisting of M coordinated cells, each of which includes one BS equipped with N_t antennas and K single-antenna users. Let i_{km} denote the index of the k th user located in the m th cell, $i_{km} = K(m-1) + k$, $m = 1, \dots, M$, $k = 1, \dots, K$. The global channel vector of user i_{km} is denoted as $\mathbf{h}_{i_{km}} = [\mathbf{h}_{i_{km}1}, \dots, \mathbf{h}_{i_{km}M}] \in \mathbb{C}^{1 \times MN_t}$, where $\mathbf{h}_{i_{km}n} = \sqrt{\alpha_{i_{km}n}} \tilde{\mathbf{h}}_{i_{km}n} \in \mathbb{C}^{1 \times N_t}$ is the sublink channel vector from the n th BS to user i_{km} , $\alpha_{i_{km}n}$ denotes the large-scale fading gain including pathloss and shadowing, and $\tilde{\mathbf{h}}_{i_{km}n} \sim \mathcal{CN}(\mathbf{0}, \tilde{\mathbf{R}}_{i_{km}n})$ is the small-scale fading channel vector following complex Gaussian distribution, $n = 1, \dots, M$.

For linear precoding, at most MN_t users can be served simultaneously. Let $\mathcal{T} = \{i_{11}, \dots, i_{KM}\}$ denote the total user pool, and $\mathcal{S} = \{s_1, \dots, s_L\}$ denote the set of indices of L scheduled users that is a subset of \mathcal{T} , i.e., $\mathcal{S} \subset \mathcal{T}$. Then the signal received by user s_l is

$$y_{s_l} = \mathbf{h}_{s_l} \mathbf{W} \mathbf{x}^T + z_{s_l}, \quad (1)$$

where $\mathbf{x} \in \mathbb{C}^{1 \times L}$ is the data symbols for the users in \mathcal{S} , z_{s_l} denotes the receiver noise and the interference from non-cooperative cells at the user s_l that is modeled as an additive white Gaussian noise (AWGN) with zero mean and variance $\sigma_{s_l}^2 = \sum_{m \in \mathcal{I}} P_m \alpha_{s_l m} + \sigma^2$, \mathcal{I} is the set of indices of non-cooperative cells, P_m is the maximal transmit power of the m th BS, and $\mathbf{W} = [\mathbf{w}_{s_1}^H, \dots, \mathbf{w}_{s_L}^H] \in \mathbb{C}^{MN_t \times L}$ is a linear precoding matrix for all scheduled users. The SINR of user s_l is

$$\gamma_{s_l} = \frac{|\mathbf{h}_{s_l} \mathbf{w}_{s_l}^H|^2}{\sum_{j \neq l} |\mathbf{h}_{s_l} \mathbf{w}_{s_j}^H|^2 + \sigma_{s_l}^2}, \quad (2)$$

where $\sum_{j \neq l} |\mathbf{h}_{s_l} \mathbf{w}_{s_j}^H|^2$ is the inter-user interference.

When perfect CSI is available, the inter-user interference can be eliminated by using zero-forcing (ZF) transmission with the precoder as [1]

$$\mathbf{W} = \mathbf{G} \mathbf{P}^{\frac{1}{2}}, \quad (3)$$

where $\mathbf{G} = \mathbf{H}_S^H (\mathbf{H}_S \mathbf{H}_S^H)^{-1}$ is the ZF beamformer (ZFBF), $\mathbf{H}_S = [\mathbf{h}_{s_1}^T, \dots, \mathbf{h}_{s_L}^T]^T$, and \mathbf{P} is a diagonal power allocation matrix. Combined with the low-complexity scheduler SUS or GUS [7, 8], the ZFBF achieves a sum rate that asymptotically grows with the number of users in the same way as dirty paper coding under sum power constraints [8, 17].

III. CHANNEL ASYMMETRY IN BS COOPERATIVE TRANSMISSION SYSTEMS

In this section, we analyze the impact of the inherent asymmetric feature of CoMP channels on the orthogonality between users by deriving the pdf of the angle between their channel vectors.

A. The Angle Between Channel Vectors of Users

Consider two users with the global channel vector \mathbf{h}_1 and \mathbf{h}_2 . Assume that the sublink small-scale fading channels are modeled as

$$\tilde{\mathbf{h}}_{im} = \mathbf{g}_{im} \tilde{\mathbf{R}}_{im}^{\frac{1}{2}}, \quad i = 1, 2, \quad m = 1, \dots, M, \quad (4)$$

where $\mathbf{g}_{im} \sim \mathcal{CN}(\mathbf{0}, \mathbf{I})$, and $\tilde{\mathbf{R}}_{im}$ is the spatial correlation matrix of the sublink channel. Then we can express the i th user's global channel vector as

$$\mathbf{h}_i = \mathbf{g}_i \mathbf{R}_i^{\frac{1}{2}}, \quad (5)$$

where $\mathbf{R}_i = \text{diag}\{[\alpha_{i1} \tilde{\mathbf{R}}_{i1}, \dots, \alpha_{iM} \tilde{\mathbf{R}}_{iM}]\}$, and $\mathbf{g}_i = [\mathbf{g}_{i1}, \dots, \mathbf{g}_{iM}]$. This shows that CoMP channels are a special kind of spatially correlated channels, which transmit correlation matrix depends on the sublink channel correlation matrices as well as the large-scale fading gains.

The angle between the two users' global channel vectors is expressed as

$$\cos^2 \theta = \frac{|\mathbf{h}_2 \mathbf{h}_1^H|^2}{\|\mathbf{h}_2\|^2 \|\mathbf{h}_1\|^2} = \frac{|\mathbf{h}_2 \mathbf{v}_1^H|^2}{\|\mathbf{h}_2\|^2}, \quad (6)$$

where $\mathbf{v}_1 = \mathbf{h}_1 / \|\mathbf{h}_1\|$. When the transmit correlation matrix is a scaled identity matrix (i.e., $\mathbf{R}_i = c\mathbf{I}$) for $i \in \{1, 2\}$, $\cos^2 \theta$ has been shown to follow a beta distribution with parameters 1 and $N - 1$ [18], where $N = MN_t$. Since CoMP channels are asymmetric, i.e., different sublink channels have different large-scale fading gains, \mathbf{R}_i is no longer a scaled identity matrix.

To obtain the pdf of $\cos^2 \theta$, we define $q_n = |\mathbf{h}_2 \mathbf{v}_n^H|^2$ and $\mathbf{q} = [q_1, \dots, q_N]$, where $\mathbf{V} = [\mathbf{v}_1^T, \mathbf{v}_2^T, \dots, \mathbf{v}_N^T]^T$ is a standard orthogonal basis generated from \mathbf{v}_1 . Then we can rewrite (6) as

$$\cos^2 \theta = \frac{q_1}{\sum_{n=1}^N q_n}. \quad (7)$$

The joint pdf of \mathbf{q} , $f_{\mathbf{q}}(\mathbf{x})$, is derived in Appendix A. By a change of variables, we can obtain the pdf of $\cos^2 \theta$ as

$$f_{\cos^2 \theta}(x) = \int_0^\infty \dots \int_0^\infty \frac{\sum_{n=2}^N y_n}{(1-x)^2} f_{\mathbf{q}} \left(\frac{x \sum_{n=2}^N y_n}{1-x}, y_2, \dots, y_N \right) dy_2 \dots dy_N. \quad (8)$$

In the following, we will use numerical results to analyze the impact of the asymmetric channel on the orthogonality between users.

B. Numerical Analysis

To highlight the impact of channel asymmetry on the orthogonality, here we take a simple but fundamental CoMP system consisting of two single-antenna BSs as an example. In this case, the channel correlation matrix of the i th user is $\mathbf{R}_i = \text{diag}\{[\alpha_{i1}, \alpha_{i2}]\}$, which depends on the user's location, $i = 1, 2$. We consider two BSs and two users that are located at the positions of $-d$, d_1 , d_2 and d , as shown in Fig. 2, $d = 250$ m. We only consider the pathloss which is set as $\alpha_{im} = -35.3 - 37.6 \log(d_{im})$ dB, where d_{im} is the distance from the m th BS to the i th user.

Figure 3 shows the pdf of $\cos^2 \theta$ with respect to different user locations (d_1, d_2) . When the users are located at the boundary of two cells, i.e., the case of $(0, 0)$, $\cos^2 \theta$ is uniformly distributed between 0 and 1. This agrees with the results in [18] since in this specific scenario the CoMP channel degenerates to a traditional single-cell channel with a two-antenna BS and the beta distribution reduces to the uniform distribution. When both users are in the same cell such as the cases of $(50, 100)$ and $(100, 100)$, $\cos^2 \theta$ has large values in a high probability. By contrast, when the two users are located in different cells such as the cases of $(-50, 100)$ and $(-100, 100)$, $\cos^2 \theta$ has small values in a high probability, i.e., the two users are more orthogonal. Resembling the single-cell MIMO systems [18], when each BS equips with more antennas, the phenomena is the same except that the users will be orthogonal with a higher probability.

IV. LOW FEEDBACK USER SCHEDULERS

We have shown that in CoMP channels user locations have large impact on the orthogonality between users. When the users are in different cells, the orthogonality depends on the large-scale fading gains, and in fact can be judged by channel norms as will be shown in this section. Otherwise, sublink small-scale channels are necessary to judge the orthogonality. This suggests the possibility of designing a low feedback scheduler to select the users with sufficient orthogonality based on user locations and channel norms. In the following, we derive several channel norm-based schedulers according to the observation. To exploit the orthogonality of users, we consider schedulers bearing the spirit of the SUS.

A. Channel Norm-based Scheduler (NUS)

Two critical factors of the SUS are the orthogonally projected norm and the orthogonal threshold [8].

In the $(l+1)$ th iteration of the SUS, we need to compute the orthogonally projected norm of the i_{km} th user's channel vector $\mathbf{h}_{i_{km}}$ onto the subspace spanned by the selected users' channel vectors \mathbf{H}_{S_l} as

$$\nu_{S_l i_{km}} = \mathbf{h}_{i_{km}} \mathbf{Q}_{i_{km}}^\perp \mathbf{h}_{i_{km}}^H, \quad (9)$$

where $\mathbf{Q}_{i_{km}}^\perp = \mathbf{I} - \mathbf{H}_{S_l}^H (\mathbf{H}_{S_l} \mathbf{H}_{S_l}^H)^{-1} \mathbf{H}_{S_l}$ is the orthogonal projection matrix, $\mathbf{H}_{S_l} = [\mathbf{h}_{s_1}^T, \dots, \mathbf{h}_{s_l}^T]^T$, $\mathbf{h}_{s_i} = [\mathbf{h}_{s_i 1}, \dots, \mathbf{h}_{s_i M}]$, $1 \leq i \leq l$, $i_{km} \in \mathcal{T}_{l+1}$, \mathcal{T}_{l+1} is the user pool in the $(l+1)$ th iteration, and $S_l = [s_1, \dots, s_l]$ is the scheduling result before the $(l+1)$ th iteration.

To obtain the orthogonally projected norm, the SUS needs full CSI from all users. In order to derive a scheduler based on channel norms, we derive a lower bound of $\nu_{S_l i_{km}}$ that only depends on the norms of the sublink channels.

Define $\Sigma = \text{diag}\{\|\mathbf{h}_{s_1}\|^2, \dots, \|\mathbf{h}_{s_l}\|^2\}$, and $\bar{\Sigma} = \mathbf{H}_{S_l} \mathbf{H}_{S_l}^H - \Sigma$. Then by using the matrix inversion lemma [19, App. A], we have

$$(\mathbf{H}_{S_l} \mathbf{H}_{S_l}^H)^{-1} = \Sigma^{-1} - \Sigma^{-1} (\Sigma^{-1} + \bar{\Sigma}^{-1})^{-1} \Sigma^{-1} \triangleq \Sigma^{-1} - \Delta. \quad (10)$$

Substituting (10) into (9), we have

$$\begin{aligned} \nu_{S_l i_{km}} &= \mathbf{h}_{i_{km}} (\mathbf{I} - \mathbf{H}_{S_l}^H (\Sigma^{-1} - \Delta) \mathbf{H}_{S_l}) \mathbf{h}_{i_{km}}^H \\ &= \mathbf{h}_{i_{km}} (\mathbf{I} - \mathbf{H}_{S_l}^H \Sigma^{-1} \mathbf{H}_{S_l}) \mathbf{h}_{i_{km}}^H + \mathbf{h}_{i_{km}} \mathbf{H}_{S_l}^H \Delta \mathbf{H}_{S_l} \mathbf{h}_{i_{km}}^H \\ &\stackrel{(a)}{\geq} \mathbf{h}_{i_{km}} (\mathbf{I} - \mathbf{H}_{S_l}^H \Sigma^{-1} \mathbf{H}_{S_l}) \mathbf{h}_{i_{km}}^H = \|\mathbf{h}_{i_{km}}\|^2 \left(1 - \sum_{j=1}^l \cos^2 \theta_{i_{km} s_j}\right), \end{aligned} \quad (11)$$

where

$$\cos \theta_{i_{km} s_j} = \frac{|\mathbf{h}_{i_{km}} \mathbf{h}_{s_j}^H|}{\|\mathbf{h}_{i_{km}}\| \|\mathbf{h}_{s_j}\|} \quad (12)$$

is the cosine of the angle between user i_{km} and user s_j , $0 \leq \theta_{i_{km} s_j} \leq \pi/2$, i.e., $\cos \theta_{i_{km} s_j} \geq 0$.

Considering the property of the inner product of vectors, $\cos \theta_{i_{km} s_j}$ is upper bounded by

$$\cos \theta_{i_{km} s_j} = \frac{|\sum_{n=1}^M \mathbf{h}_{i_{km} n} \mathbf{h}_{s_j n}^H|}{\sqrt{\sum_{n=1}^M \|\mathbf{h}_{i_{km} n}\|^2} \sqrt{\sum_{n=1}^M \|\mathbf{h}_{s_j n}\|^2}} \stackrel{(b)}{\leq} \frac{\sum_{n=1}^M \|\mathbf{h}_{i_{km} n}\| \|\mathbf{h}_{s_j n}\|}{\sqrt{\sum_{n=1}^M \|\mathbf{h}_{i_{km} n}\|^2} \sqrt{\sum_{n=1}^M \|\mathbf{h}_{s_j n}\|^2}} \triangleq \mu_{i_{km} s_j}, \quad (13)$$

then we get the lower bound of the orthogonally projected norm as

$$\nu_{S_l i_{km}} \stackrel{(c)}{\geq} \|\mathbf{h}_{i_{km}}\|^2 \left(1 - \sum_{j=1}^l \mu_{i_{km} s_j}^2\right) \triangleq \nu_{S_l i_{km}}^{lb}. \quad (14)$$

One can see that $\nu_{S_l i_{km}}^{lb}$ only depends on the norms of the sublink channels from cooperative BSs. Assuming homogeneous users, the SUS selects users merely based on $\nu_{S_l i_{km}}$ [8]. Since in CoMP systems we need to consider heterogeneous users which experience different interference from non-cooperative BSs, we select users based on the term $\nu_{S_l i_{km}}^{lb} / \sigma_{i_{km}}^2$, which reflects the receive signal-to-noise ratio (SNR) with ZFBF.

As a successive user scheduler, the SUS terminates the scheduling procedure by controlling the orthogonality between the selected users. Analogously, we introduce a threshold ϵ to ensure $\mu_{i_{km} s_j} \leq \epsilon$, i.e, we restrict the upper bound of $\cos \theta_{i_{km} s_j}$. This is equivalent to introduce a constraint on the lower bound of the angle between the channel vectors of the two users.

Now we consider the tightness of the lower bound $\nu_{S_l i_{km}}^{lb}$ and the upper bound $\mu_{i_{km} s_j}$ by analyzing the tightness of the three inequalities (a), (b) and (c) in (11), (13) and (14).

The equality of (a) holds when $\Delta = \mathbf{0}$. This implies that the users in S_l are orthogonal among each other since in this case $\mathbf{H}_{S_l} \mathbf{H}_{S_l}^H = \Sigma$ is diagonal according to (10). In the proposed NUS, the scheduled users are semi-orthogonal which is ensured by judiciously choosing the threshold ϵ . Thereby the gap of the two terms in the left and right hand sides of inequality (a) is small.

By examining inequality (b), we will see that the tightness of $\mu_{i_{km} s_j}$ depends on the users' location. In the first case, when user i_{km} and the selected users in S are in different cells, $\mu_{i_{km} s_j}$ is tight. To see this, noting that the signals from non-local BSs experience much stronger attenuation, at least one of the two terms, $\|\mathbf{h}_{i_{km} n}\|$ and $\|\mathbf{h}_{s_j n}\|$, will be very small, and hence $\mu_{i_{km} s_j}$ is small. Considering inequality (b) and the fact that $\cos \theta_{i_{km} s_j} \geq 0$, we have $\mu_{i_{km} s_j} - \cos \theta_{i_{km} s_j} \leq \mu_{i_{km} s_j}$, which means that $\mu_{i_{km} s_j}$ is a tight upper bound of $\cos \theta_{i_{km} s_j}$. Further considering inequality (c), we know that $\nu_{S_l i_{km}}^{lb}$ is also a tight lower bound. In the second case, when user i_{km} and user s_j are in the m th cell, both $\|\mathbf{h}_{i_{km} n}\|$ and $\|\mathbf{h}_{s_j n}\|$ will be very small for $n \neq m$. Then we can ignore all other $M - 1$ terms in the sum of the numerator in (13) except for the term with $n = m$, and the tightness of $\mu_{i_{km} s_j}$ can be approximately reflected by $\|\mathbf{h}_{i_{km} m}\| \|\mathbf{h}_{s_j m}\| - |\mathbf{h}_{i_{km} m} \mathbf{h}_{s_j m}^H|$. It is zero if every BS has only one antenna, then $\mu_{i_{km} s_j}$ is tight. Otherwise, $\mu_{i_{km} s_j}$ is not tight since $|\mathbf{h}_{i_{km} m} \mathbf{h}_{s_j m}^H|$ may be zero when the small-scale fading channels are orthogonal, thereby $\nu_{S_l i_{km}}^{lb}$ is not tight as well. However, we know from the numerical results in Fig. 3 that the angle between two users in the same cell is small with a high probability. Therefore, $\mu_{i_{km} s_j}$ is often too large to satisfy the orthogonality constraint. This implies that the NUS will select same-cell users with a low probability. We will show the

tightness of the lower bound through numerical analysis in section VI.

Let \mathcal{T}_l and \mathcal{S}_l denote the user pool and the scheduling result at the l th step, and set $\mathcal{T}_0 = \{1, 2, \dots, MK\}$, then the NUS is summarized as follows.

- 1) Initialize by selecting a user with the maximum SNR as the first user,

$$s_1 = \arg \max_{i_{km} \in \mathcal{T}_0} \frac{\|\mathbf{h}_{i_{km}}\|^2}{\sigma_{i_{km}}^2}. \quad (15)$$

Set $\mathcal{S}_1 = \{s_1\}$ and $l = 1$.

- 2) When $l \leq \min(MN_t, MK)$, obtain the user pool \mathcal{T}_l as

$$\mathcal{T}_l = \{i_{km} \in \mathcal{T}_{l-1}, i_{km} \notin \mathcal{S}_l \mid \mu_{i_{km}s_l} \leq \epsilon\}. \quad (16)$$

If $\mathcal{T}_l = \phi$ (empty set), the iteration will stop. Otherwise, compute the lower bound $\nu_{\mathcal{S}_l i_{km}}^{lb}$ of the orthogonally projected norm and select the user with the largest $\nu_{\mathcal{S}_l i_{km}}^{lb} / \sigma_{i_{km}}^2$,

$$s_{l+1} = \arg \max_{i_{km} \in \mathcal{T}_l} \frac{\nu_{\mathcal{S}_l i_{km}}^{lb}}{\sigma_{i_{km}}^2}. \quad (17)$$

Set $\mathcal{S}_{l+1} = \mathcal{S}_l \cup \{s_{l+1}\}$ and $l = l + 1$, where \cup denotes the union between two sets.

We next discuss the selection of the orthogonality threshold ϵ by analyzing its influence on the performance. With the full CSI, the SNR of the selected user s_{l+1} under ZF precoding is

$$\gamma_{s_{l+1}} = \frac{p_{s_{l+1}} \nu_{\mathcal{S}_l s_{l+1}}}{\sigma_{s_{l+1}}^2}, \quad (18)$$

where $p_{s_{l+1}}$ is the allocated power to the user s_{l+1} . The SNR can be lower bounded by

$$\gamma_{s_{l+1}} \geq \frac{p_{s_{l+1}} \nu_{\mathcal{S}_l s_{l+1}}^{lb}}{\sigma_{s_{l+1}}^2} = p_{s_{l+1}} \max_{i_{km} \in \mathcal{T}_l} \frac{\nu_{\mathcal{S}_l i_{km}}^{lb}}{\sigma_{i_{km}}^2} \quad (19)$$

since $\nu_{\mathcal{S}_l s_{l+1}}^{lb}$ is the lower bound of $\nu_{\mathcal{S}_l s_{l+1}}$ and the user is selected according to (17). Considering that $\mu_{i_{km}s_j} \leq \epsilon$ for all $i_{km} \in \mathcal{T}_l$, according to (14) the SNR can be further lower bounded by

$$\gamma_{s_{l+1}} \geq p_{s_{l+1}} (1 - l\epsilon^2) \max_{i_{km} \in \mathcal{T}_l} \frac{\|\mathbf{h}_{i_{km}}\|^2}{\sigma_{i_{km}}^2}. \quad (20)$$

It follows that the threshold ϵ has an intertwined impact on the performance. On one hand, the non-orthogonality between users reduces the receive power which is reflected in the term $\sum_{j=1}^l \cos^2 \theta_{i_{km}s_j}$ in (11). Consider that $\cos \theta_{i_{km}s_j} \leq \mu_{i_{km}s_j} \leq \epsilon$, such a reduction is upper bounded by $l\epsilon^2$, which becomes negligible if ϵ is small enough. On the other hand, multiuser diversity gain achieved by user s_{l+1} depends on the size of \mathcal{T}_l from which user s_{l+1} is selected. Since the

elements in \mathcal{T}_l satisfy the orthogonality constraint in (16), a large threshold should be chosen to ensure a large user candidate pool.

When the NUS is applied in a network (M, N_t, K) , each user to be scheduled only needs to feed back M real scalars to the coordinated BSs at each time slot. Only the selected users need to provide their channel vectors to the BSs for precoding.

B. Local Channel Aided NUS (LocalNUS)

As analyzed earlier, the channel norm provides sufficient information for judging the orthogonality between users only when they are not located in the same cell. As a result, the NUS is prone to select users located in different cells even when the small-scale fading channels of some users in a cell have good orthogonality. This will decrease the multiuser diversity gain, which can be overcome by a scheduler with the aid of full local channels.

We have found that the upper bound $\mu_{i_k m s_j}$ in the NUS is not tight for two users located in the same cell, which is caused by amplifying $|\mathbf{h}_{i_k m} \mathbf{h}_{s_j m}^H|$ to $\|\mathbf{h}_{i_k m}\| \|\mathbf{h}_{s_j m}\|$. If all users can feed back their local channels, we can compute $|\mathbf{h}_{i_k m} \mathbf{h}_{s_j m}^H|$, and thereby a tighter upper bound of $\cos \theta_{i_k m s_j}$ can be achieved as

$$\cos \theta_{i_k m s_j} \leq \frac{\sum_{\substack{n=1 \\ n \neq m}}^M \|\mathbf{h}_{i_k m n}\| \|\mathbf{h}_{s_j n}\| + t}{\sqrt{\sum_{n=1}^M \|\mathbf{h}_{i_k m n}\|^2} \sqrt{\sum_{n=1}^M \|\mathbf{h}_{s_j n}\|^2}} \triangleq \bar{\mu}_{i_k m s_j}, \quad (21)$$

where $t = |\mathbf{h}_{i_k m} \mathbf{h}_{s_j m}^H|$ if user s_j is also in the m th cell; otherwise $t = \|\mathbf{h}_{i_k m}\| \|\mathbf{h}_{s_j m}\|$ since $\mathbf{h}_{s_j m}$ is still not available in this case.

By updating the $\mu_{i_k m s_j}$ and the corresponding $\nu_{S_l i_k m}^{lb}$ with $\bar{\mu}_{i_k m s_j}$ in the procedure of the NUS, we get a new scheduler which is named LocalNUS. To apply the LocalNUS, each user needs to feed back the full local channel and $M - 1$ norms of cross channels at each time slot.

C. Large-scale Fading based Scheduler (LUS)

With the NUS and the LocalNUS, the two-phase transmit strategy can effectively reduce the feedback overhead. However, scheduling delay is induced which will degrade the performance in time-varying channels.

We propose a quasi-static scheduler to solve this problem. Considering the fact that the channel norm is dominated by the large-scale fading gain, then by replacing the square norms of sublink

channels $\|\mathbf{h}_{i_{km}n}\|^2$ in (13) and (14) with the corresponding large-scale fading gains $\alpha_{i_{km}n}$, the upper bound $\mu_{i_{km}s_j}$ and the lower bound $\nu_{S_{l i_{km}}}^{lb}$ can be approximately expressed as

$$\bar{\mu}_{i_{km}s_j} = \frac{\sum_{n=1}^M \sqrt{\alpha_{i_{km}n} \alpha_{s_j n}}}{\sqrt{\sum_{n=1}^M \alpha_{i_{km}n}} \sqrt{\sum_{n=1}^M \alpha_{s_j n}}} \text{ and } \bar{\nu}_{S_{l i_{km}}}^{lb} = \alpha_{i_{km}} \left(1 - \sum_{j=1}^l \bar{\mu}_{i_{km}s_j}^2 \right). \quad (22)$$

By applying $\bar{\mu}_{i_{km}s_j}$ and $\bar{\nu}_{S_{l i_{km}}}^{lb}$ in the procedure of the NUS, we obtain a large-scale fading gain based scheduler, called LUS. Since the large-scale fading gain varies very slowly, all users only need to feed back their large-scale fading gains in a very low rate.

It should be noted that the quasi-static LUS is only applicable for the systems with asymmetric channels. When the LUS is used in single-cell systems, it is equivalent to select the users with the largest average channel gains which generally does not perform well, since the orthogonality between users is independent of their large-scale fading gains in this case.

D. The Fairness Issues

The schedulers considered so far favor users with good channel conditions, which follows from the selection criterion of (17). As a result, only users at the cell center will be served, which contradicts to the goal of CoMP to improve the cell-edge throughput. This can be solved by combining the proposed schedulers with fair scheduling algorithms such as Round-robin (RR) or proportional fair scheduler.

To demonstrate the performance of the proposed schedulers in CoMP systems, we extend them in a RR fashion similar to [8, 20], named the RR-NUS, the RR-LocalNUS and the RR-LUS, respectively. They select a group of users at each time slot and remove the selected users from the user pool at next time slot. The RR-LUS can be quasi-statically performed over a relatively long period, during which the pre-selected users feed back their CSI for precoding at each time slot. Since equal time slots are allocated to all the users, a short-term fairness is guaranteed [20].

V. FEEDBACK OVERHEAD COMPARISON

A. Channel Quantization Model

We consider quantized feedback to provide CSI at BSs with the following assumptions.

Assumption 1: Each user has perfect downlink channels.

We express the sublink channel from the m th BS to the i th user as $\mathbf{h}_{im} = \rho_{im} \mathbf{v}_{im}$, where ρ_{im} is the norm of \mathbf{h}_{im} referred to as the CQI and $\mathbf{v}_{im} = \mathbf{h}_{im} / \|\mathbf{h}_{im}\|$ is the CDI. Since the

global CoMP channel vector of each user consists of the sublink channel vectors from multiple coordinated BSs, we make the following assumption.

Assumption 2: The CDI of the sublink channel vector from every coordinated BS is individually quantized for each user. The i th user quantizes \mathbf{v}_{im} to a unit norm vector chosen from a codebook $\mathbf{C}_{im} = [\mathbf{c}_{im,1}^H, \dots, \mathbf{c}_{im,J}^H]^H$ according to the minimum distance criterion

$$j_{im} = \arg \min_{j=1,\dots,J} |\mathbf{v}_{im} \mathbf{c}_{im,j}^H|, \quad m = 1, \dots, M, \quad J = 2^B. \quad (23)$$

In order to avoid the same channel quantization for different users, the codebook should be user specific. Here we consider a correlated random codebook \mathbf{C}_{im} shown in [21], in which the unit norm vectors are generated by $\mathbf{c}_{im,j} = \mathbf{e}_{im,j} / \|\mathbf{e}_{im,j}\|$ with correlated complex Gaussian random vectors $\mathbf{e}_{im,j} \sim \mathcal{CN}(\mathbf{0}, \tilde{\mathbf{R}}_{im})$ for $j \in \{1, \dots, J\}$, where $\tilde{\mathbf{R}}_{im}$ is the correlation matrix of the small-scale sublink channel $\tilde{\mathbf{h}}_{im}$.

The codebook \mathbf{C}_{im} is predefined and known by both the i th user and the coordinated BSs. The i th user feeds back the selected codebook indices to its local BS, each with B bits. Apart from the CDI, the CQI should also be quantized and sent back. Due to the ease of quantizing a scalar ρ_{im} , we make the third assumption as in [15] and [18].

Assumption 3: The CQI is perfectly known to the BSs through feedback.

With the feedback for both the CDI and the CQI, the BSs can reconstruct the global channel vector of the i th user as $\hat{\mathbf{h}}_i = [\hat{\mathbf{h}}_{i1}, \dots, \hat{\mathbf{h}}_{iM}]$ with $\hat{\mathbf{h}}_{im} = \rho_{im} \mathbf{c}_{im,j_{im}}$. Based on the reconstructed channels, scheduling, ZF beamforming and power allocation can be conducted.

To achieve a close approximation of the channel vector, a large-size codebook is generally necessary, which however is unaffordable in practical systems due to the huge feedback overhead. In practice, the number of feedback bits per user is limited not only by the capacity of its own feedback link [15], but also by the capacity of the system feedback channel that is shared by all users [16]. Therefore, two constraints with respect to the size of the codebook are considered in this paper. We limit the number of feedback bits per user to B_u for quantizing M sublink channels, and also limit the total number of feedback bits from all users to B_t .

B. Feedback Overhead with Different Schedulers

Based on the channel quantization model, we analyze the codebook size when different schedulers are employed given the per-user and total feedback constraints, B_u and B_t .

Both the GUS and the SUS are designed for the systems with one-phase strategy, which require all users to feed back the quantized channels for scheduling and precoding. The size of the codebook, B , should satisfy that $MB \leq B_u$ and $M^2KB \leq B_t$, i.e., $B \leq \min(\frac{B_u}{M}, \frac{B_t}{KM^2})$.

The proposed schedulers are designed for the system with two-phase strategy. For the NUS, at each time slot each user needs to feed back M real scalars (i.e., CQI) to the coordinated BSs. In addition the selected L users need to provide the channels for precoding. If we neglect the overhead for feeding back scalars, the size of the codebook should satisfy $B \leq \min(\frac{B_u}{M}, \frac{B_t}{ML})$. For the LocalNUS, at each time slot each user needs to provide the channel vectors of local channels and the CQI of cross channels, and then the selected L users need to feed back the channel vectors. The size of the codebook should satisfy $B \leq \min(\frac{B_u}{M}, \frac{B_t}{MK+ML})$. For the LUS, the feedback overhead for large-scale fading gain is negligible, and at each time slot the L selected users feed back their channel vectors, which leads to a codebook size of $B \leq \min(\frac{B_u}{M}, \frac{B_t}{ML})$.

The feedback overhead of different schedulers given the size of the codebook, as well as the size of the codebook given the per-user and total feedback constraints is summarized in Table I. Note that the number of the scheduled users L for different schedulers differs.

VI. SIMULATION RESULTS

In this section, we analyze the tightness of the lower bounds derived previously and evaluate the performance of the proposed schedulers via Monte-Carlo simulations. Except for the RR-NUS, the RR-LocalNUS and the RR-LUS, three relevant user schedulers, the RR-RUS (random user scheduler [12, 13]), the RR-GUS and the RR-SUS are also considered for comparison. Similar to the RR-NUS, they select a group of users to be served at each time slot according to the RUS, the GUS and the SUS, respectively. The ZFBF together with the optimal power allocation to maximize the achievable sum rate under PBPC is used for all schemes. The GUS under PBPC is extended from the scheduler proposed in [22]. Assume that a scheduling period of RR-based schedulers consists of Q time slots, in other words, the total user pool is divided into Q user groups. Since the scheduling period of different schedulers differs, we will use Q to normalize the user's throughput in following performance evaluations.

With the same system model and parameters as in Section III-B except for each BS having two antennas in order to analyze the impact of local channels, we show the tightness of $\nu_{S_{l i_{km}}}^{lb}$ with respect to the position of user i_{km} denoted by d_2 in Fig. 4. We take the normalized gap

between $\nu_{S_l i_{km}}$ and $\nu_{S_l i_{km}}^{lb}$ as the metric, which is defined as $(\nu_{S_l i_{km}} - \nu_{S_l i_{km}}^{lb}) / \nu_{S_l i_{km}}$. We consider the case that S_l includes one user located at the position of $d_1 = -50$ m. It is shown that $\nu_{S_l i_{km}}^{lb}$ is not tight for the NUS and the LUS when $d_2 < 0$, i.e., when the two users are in the same cell, and the largest gap occurs when the two users are at the same position. With the aid of local channels, the bound is tightened. As a result, the LocalNUS can improve performance significantly, which will be shown in the sequel. However, when user i_{km} is located at the cell edge, the bounds are still loose.

The simulation setup is based on [23]. In particular, we consider a CoMP system consisting of 3 coordinated cells surrounded by interfering cells as shown in Fig. 5. The interference from the non-cooperative cells is modeled as white noise. The BS-to-BS distance is 500 m, and the channel bandwidth is 10 MHz. The BSs transmit with a maximal power of 40 Watts, and the users have a receiver noise figure of 9 dB. The path loss exponent is 3.76, the lognormal shadowing standard deviation is 8 dB, and the mean power loss at the reference distance of 1 m is 36.3 dB. The BS is equipped with a 4-antenna uniform linear array with half a wavelength antenna separation. Each cell has 20 uniformly distributed single-antenna users that are surrounded by rich scatterers and keep a minimum distance of 35 m from the BS. For each drop of users, the small-scale fading channels are modeled as Rayleigh fading with correlation at the transmitter side. The correlation matrix is generated following the single-bounce model [24], where the angular spread of the Gaussian distributed scatterers at the user side is assumed to be 15 degrees unless otherwise specified. In the scenario of limited feedback, the correlation matrix is assumed to be known *a priori* for codebook generation. All the results are averaged over 100 drops.

In Fig. 6, we plot the cell-average throughput and the cell-edge throughput¹ achieved by each individual user using ZF precoding together with the RR-NUS, the RR-LocalNUS and the RR-LUS subject to the PBPC, as a function of the threshold ϵ used in the three schedulers. We can see that both the cell-average and the cell-edge throughput are not a monotonic function of ϵ for three schedulers. This is led by the complicate influence of ϵ on the performance. As have analyzed earlier, at each time slot ϵ will not only affect the user's receive power, but also affect the multiuser diversity gain. These two effects of ϵ are counteracting, which should be

¹The cell-edge throughput is defined as the 5% point of the cumulative distribution function (CDF) of the user throughput normalized by channel bandwidth [25]. In the simulations, the normalized user throughput is obtained via the Shannon capacity formula.

considered for selecting ϵ . Besides, for a given total user number, the scheduling period of RR-based schedulers depends on the number of selected users at each time slot, which is determined by ϵ . Again, this shows that the selection of ϵ is not explicit. From the figure, the threshold of the RR-NUS, the RR-LocalNUS and the RR-LUS can be respectively chosen as 0.4, 0.8 and 0.8 to achieve high cell-average and cell-edge throughput.

Figure 7 shows the CDF of user throughput of the six schedulers when perfect CSI is assumed for precoding, where the RR-GUS and the RR-SUS use the perfect CSI, and the RR-NUS or the RR-LocalNUS only use perfect channel norm or perfect local channel and the norms of cross channels. Compared with the RR-RUS, other advanced schedulers show the obvious performance gain. At each time slot, the RR-RUS randomly serves as many users as possible because it has no criterion to determine the number of selected users, which leads to the shortest scheduling period. Despite that the RR-RUS may select a few high-rate users, the severe inter-user interference led by random grouping degrades most users' performance. The RR-GUS and the RR-SUS have high throughput due to the perfect knowledge of CSI at the BSs. The RR-NUS effectively reduces the feedback overhead but pays a performance penalty. Nevertheless, the gap between the RR-NUS and the RR-GUS/SUS is recovered by the RR-LocalNUS with additional feedback of local channel. The performance of the RR-LUS is slightly inferior to that of the RR-NUS, since the channel norms are dominated by the large-scale fading gains. We can see the impact of the tightness of $\nu_{S_{lkm}}^{lb}$ on the performance. Since the bounds are loose for cell-edge users, the channel norm-based schedulers intend to use single-user MIMO precoding to serve these users. This reduces the multiuser multiplexing gain and prolongs the scheduling period. As a result, the user throughput reduces.

The performance of the six schedulers with limited feedback is shown in Fig. 8 and Fig. 9, where the angular spread at the user side is set to be 15 degrees and 35 degrees, which are the typical values usually considered in the evaluation [23]. To separate the impact of the special spatial correlation led by the channel asymmetry from the impact of the sublink channel correlation led by small angular spread, we also provide results for the channel with 360-degree angular spread which is in fact uncorrelated in Fig. 10. We limit the number of feedback bits for quantizing each sublink channel to be 4, which results in the maximal number of feedback bits per user as $B_u = 12$. To reflect the constraint on the total number of bits for all users, we set $B_t = 0.6MKB_u$ in the simulation. From the figures we see that decreasing the angular spread results

in an improvement of throughput. This is because the considered correlated random codebook reduces the quantization error of the channels with small angular spread, which is observed in [26]. Compared with the case of perfect CSI in Fig. 7, it is shown that limited feedback with few bits largely affects the relationship between the RR-NUS and the RR-GUS/SUS. The gap between the RR-NUS and the RR-GUS/SUS is small for the angular spread of 15 degrees in Fig. 8, and the RR-NUS performs the best for the angular spread of 35 and 360 degrees in Fig. 9 and Fig. 10. This is because the RR-NUS has the largest codebook for channel quantization as shown in Table I which provides a better precoder for mitigating inter-user interference.

Finally, the impact of time-varying channels on the performance of the schedulers is shown in Fig. 11. The scheduling delay of one time slot of 5 ms is considered. The time-varying channels are generated based on Jakes' model [27]. As expected, the time-varying channels degrade the performance of the RR-NUS and the RR-LocalNUS due to scheduling delay, but have no impact on the performance of the quasi-static RR-LUS.

VII. CONCLUSION

We have studied low feedback user scheduling for CoMP MU-MIMO systems in this paper.

By characterizing the statistics of the angle between two users' channel vectors and analyzing the tightness of a lower bound of the orthogonally projected norm, we have shown that the inherent asymmetric feature of CoMP channels enables the channel norm to provide sufficient information on determining the orthogonality between users. Based on this observation, we have proposed a channel norm-based user scheduler (NUS) and an enhanced local-channel aided NUS (LocalNUS). To reduce the scheduling delay of the two schedulers, we have proposed a quasi-static scheduler using large-scale fading gain (LUS). Simulation results show that the LocalNUS has fairly good performance with much less feedback overhead than the GUS and the SUS with perfect CSI, the NUS performs very close to or even better than the GUS and the SUS when limited feedback is considered, and the LUS performs well in time-varying channels.

The proposed schedulers are applicable to both the downlink BS cooperative transmission systems and the distributed antenna systems, as well as BS and relay cooperative systems, where the channels exhibit asymmetric feature.

APPENDIX A

JOINT PDF OF \mathbf{q}

We first investigate the pdf of \mathbf{v}_1 , then with the derivation of the conditional joint pdf of \mathbf{q} given \mathbf{v}_1 , $f_{\mathbf{q}}(\mathbf{x})$ can be obtained according to the Bayes' rule.

Define $\mathbf{h}_1 = [\sqrt{\xi_1}e^{j\phi_1}, \dots, \sqrt{\xi_N}e^{j\phi_N}]$ and $\eta = \|\mathbf{h}_1\|^2 = \sum_{n=1}^N \xi_n$. Then \mathbf{v}_1 can be expressed as $\mathbf{v}_1 = [\sqrt{\delta_1}e^{j\phi_1}, \dots, \sqrt{\delta_N}e^{j\phi_N}]$ with $\delta_n = \xi_n/\eta$, where $0 \leq \delta_n \leq 1$, $0 \leq \phi_n \leq 2\pi$, $n = 1, \dots, N$, and $\delta_N = 1 - \sum_{n=1}^{N-1} \delta_n$.

The joint pdf of η , $\boldsymbol{\xi}$ and $\boldsymbol{\phi}$, $f_{\eta, \boldsymbol{\xi}, \boldsymbol{\phi}}(x, \mathbf{y}, \mathbf{z})$, is given in [28], where $\boldsymbol{\xi} = [\xi_1, \dots, \xi_{N-1}]$ and $\boldsymbol{\phi} = [\phi_1, \dots, \phi_N]$, from which we can obtain the joint pdf of $\boldsymbol{\delta}$ and $\boldsymbol{\phi}$ as

$$f_{\boldsymbol{\delta}, \boldsymbol{\phi}}(\mathbf{y}, \mathbf{z}) = \int_0^\infty x^{N-1} f_{\eta, \boldsymbol{\xi}, \boldsymbol{\phi}}(x, \mathbf{y}, \mathbf{z}) dx, \quad (24)$$

where $\boldsymbol{\delta} = [\delta_1, \dots, \delta_{N-1}]$, and x^{N-1} is the Jacobian determinant.

Given $\boldsymbol{\delta}$ and $\boldsymbol{\phi}$ (i.e., given \mathbf{v}_1), it is not hard to find that the vector $[\mathbf{h}_2 \mathbf{v}_1^H, \dots, \mathbf{h}_2 \mathbf{v}_N^H]$ follows the joint complex Gaussian distribution $\mathcal{CN}(\mathbf{0}, \mathbf{V} \mathbf{R}_2 \mathbf{V}^H)$. Note that $q_n = |\mathbf{h}_2 \mathbf{v}_n^H|^2$, $n = 1, \dots, N$. Then by following the work in [29], we can get the conditional joint pdf of \mathbf{q} given $\boldsymbol{\delta}$ and $\boldsymbol{\phi}$ as

$$f_{\mathbf{q}|\boldsymbol{\delta}, \boldsymbol{\phi}}(\mathbf{q}) = \sum_{r=0}^{\infty} \frac{(1/2)_r}{r!} \frac{e^{-\sum_{n=1}^N \frac{q_n}{a_{nn}}}}{\prod_{n=1}^N a_{nn}} \left(1 - \sum_{n_1, \dots, n_N=0}^2 C_{n_1, \dots, n_N} \left[\frac{L(\frac{q_1}{a_{11}})}{a_{11}} \right]^{n_1} \cdots \left[\frac{L(\frac{q_N}{a_{NN}})}{a_{NN}} \right]^{n_N} \right)^r, \quad (25)$$

where the operator $(x)_r = x(x+1) \dots (x+r-1)$, the function $L(x)$ satisfies

$$[L(x)]^m [L(x)]^n = [L(x)]^{m+n} \quad \text{and} \quad [L(x)]^m \equiv L_m(x), \quad (26)$$

and $L_m(x)$ is the Laguerre polynomials of degree m [30, (8.970)]. C_{n_1, \dots, n_N} is the Taylor expansion coefficient of $g(\boldsymbol{\beta}) = \left| \begin{smallmatrix} \tilde{\mathbf{A}} & \tilde{\mathbf{B}} \\ -\tilde{\mathbf{B}} & \tilde{\mathbf{A}} \end{smallmatrix} \right|$ around the point $\boldsymbol{\beta} = [\beta_1, \dots, \beta_N] = \mathbf{0}$, which is

$$C_{n_1, \dots, n_N} = (n_1! \dots n_N!)^{-1} \frac{\partial^{n_1 + \dots + n_N} g}{\partial \beta_1^{n_1} \dots \partial \beta_N^{n_N}}, \quad (27)$$

where

$$\tilde{\mathbf{A}} = \begin{bmatrix} 1 & a_{12}\beta_2 & \dots & a_{1N}\beta_N \\ a_{21}\beta_1 & 1 & \dots & a_{2N}\beta_N \\ \vdots & \vdots & \ddots & \vdots \\ a_{N1}\beta_1 & a_{N2}\beta_2 & \dots & 1 \end{bmatrix}, \quad \tilde{\mathbf{B}} = \begin{bmatrix} 0 & b_{12}\beta_2 & \dots & b_{1N}\beta_N \\ b_{21}\beta_1 & 0 & \dots & b_{2N}\beta_N \\ \vdots & \vdots & \ddots & \vdots \\ b_{N1}\beta_1 & b_{N2}\beta_2 & \dots & 0 \end{bmatrix},$$

and a_{ij} and b_{ij} respectively denote the element at i th row and j th column of $\Re\{\mathbf{V} \mathbf{R}_2 \mathbf{V}^H\}$ and $\Im\{\mathbf{V} \mathbf{R}_2 \mathbf{V}^H\}$ for $i, j \in \{1, \dots, N\}$.

Based on (24) and (25), we can obtain the joint pdf of \mathbf{q} as

$$f_{\mathbf{q}}(\mathbf{x}) = \int_{0 \leq z_1, \dots, z_N \leq 2\pi} \int_{y_1 + \dots + y_{N-1} \leq 1} f_{\mathbf{q}|\delta, \phi}(\mathbf{x}) f_{\delta, \phi}(\mathbf{y}, \mathbf{z}) d\mathbf{y} d\mathbf{z}. \quad (28)$$

It should be noted that the values of \mathbf{q} are not completely determined by \mathbf{v}_1 , since the standard orthogonal basis \mathbf{V} generated from \mathbf{v}_1 is not unique. However, different \mathbf{V} will lead to the same angle as $\cos^2 \theta = q_1 / \|\mathbf{h}_2\|^2$. Therefore, to obtain the joint pdf of \mathbf{q} from (28) we only need to consider a specific \mathbf{V} generated from \mathbf{v}_1 , e.g., by means of the Gram-Schmidt process.

REFERENCES

- [1] K. Karakayali, G. Foschini, and R. Valenzuela, "Network coordination for spectrally efficient communications in cellular systems," *IEEE Wireless Commun. Mag.*, vol. 13, pp. 56–61, Aug. 2006.
- [2] A. Tölli, M. Codreanu, and M. Juntti, "Cooperative MIMO-OFDM cellular system with soft handover between distributed base station antennas," *IEEE Trans. Wireless Commun.*, vol. 7, pp. 1428–1440, Apr. 2008.
- [3] H. Zhang, N. B. Mehta, A. F. Molisch, J. Zhang, and H. Dai, "Asynchronous interference mitigation in cooperative base station systems," *IEEE Trans. Wireless Commun.*, vol. 7, pp. 155–165, Jan. 2008.
- [4] H. Huang, M. Trivellato, A. Hottinen, M. Shafi, P. Smith, and R. A. Valenzuela, "Increasing downlink cellular throughput with limited network MIMO coordination," *IEEE Trans. Wireless Commun.*, vol. 8, pp. 2983–2989, 2009.
- [5] W. Choi and J. G. Andrews, "The capacity gain from intercell scheduling in multi-antenna systems," *IEEE Trans. Wireless Commun.*, vol. 7, pp. 714–725, Feb. 2008.
- [6] R. Bhagavatula, R. W. Heath Jr., and B. Rao, "Limited feedback with joint CSI quantization for multicell cooperative generalized eigenvector beamforming," in *Proc. IEEE Int. Conf. Acoust., Speech and Sig. Proc. (ICASSP)*, 2010.
- [7] G. Dimic and N. D. Sidiropoulos, "On downlink beamforming with greedy user selection: performance analysis and a simple new algorithm," *IEEE Trans. Signal Processing*, vol. 53, pp. 3857–3868, Oct. 2005.
- [8] T. Yoo and A. Goldsmith, "On the optimality of multiantenna broadcast scheduling using zero-forcing beamforming," *IEEE J. Select. Areas Commun.*, vol. 24, pp. 528–541, Mar. 2006.
- [9] T. Yoo, N. Jindal, and A. Goldsmith, "Multi-antenna downlink channels with limited feedback and user selection," *IEEE J. Select. Areas Commun.*, vol. 25, pp. 1478–1491, Sept. 2007.
- [10] D. Hammarwall, M. Bengtsson, and B. Ottersten, "Utilizing the spatial information provided by channel norm feedback in SDMA systems," *IEEE Trans. Signal Processing*, vol. 56, pp. 3278–3293, July 2008.
- [11] R. Zakhour and D. Gesbert, "A two-stage approach to feedback design in multi-user MIMO channels with limited channel state information," in *Proc. IEEE Int. Symp. Personal, Indoor Mobile Radio Commun. (PIMRC)*, 2007.
- [12] X. Zhang, E. Jorswieck, B. Ottersten, and A. Paulraj, "User selection schemes in multiple antenna broadcast channels with guarantee performance," in *Proc. IEEE Workshop on Signal Processing Advances in Wireless Commun. (SPAWC)*, 2007.
- [13] —, "On the optimality of opportunistic beamforming with hard SINR constraints," *EURASIP Journal on Advances in Signal Processing*, 2009. [Online]. Available: <http://www.hindawi.com/journals/asp/2009/475273.html>
- [14] D. Love, R. Heath Jr., V. K. N. Lau, D. Gesbert, B. D. Rao, and M. Andrews, "An overview of limited feedback in wireless communication systems," *IEEE J. Select. Areas Commun.*, vol. 26, pp. 1341–1365, Oct. 2008.

- [15] K. Huang, J. G. Andrews, and R. W. Heath Jr., “Performance of orthogonal beamforming for SDMA with limited feedback,” *IEEE Trans. Veh. Technol.*, vol. 58, pp. 152–164, Jan. 2009.
- [16] K. Huang, R. W. Heath Jr., and J. G. Andrews, “Space division multiple access with a sum feedback rate constraint,” *IEEE Trans. Signal Processing*, vol. 55, pp. 3879–3891, July 2007.
- [17] J. Q. Wang, D. J. Love, and M. D. Zoltowski, “User selection with zero-forcing beamforming achieves the asymptotically optimal sum rate,” *IEEE Trans. Signal Processing*, vol. 56, pp. 3713–3726, Aug. 2008.
- [18] N. Jindal, “MIMO broadcast channels with finite rate feedback,” *IEEE Trans. Inform. Theory*, vol. 52, pp. 5045–5060, Nov. 2006.
- [19] H. L. V. Trees, *Optimum Array Processing, Part IV of Detection, Estimation and Modulation Theory*. Wiley, 2002.
- [20] S. S. Kulkarni and C. Rosenberg, “Opportunistic scheduling policies for wireless systems with short term fairness constraint,” in *Proc. IEEE Glob. Telecom. Conf. (GLOBECOM)*, 2003.
- [21] F. Kaltenberger, M. Kountouris, D. Gesbert, and R. Knopp, “Performance of multi-user MIMO precoding with limited feedback over measured channels,” in *Proc. IEEE Glob. Telecom. Conf. (GLOBECOM)*, 2008.
- [22] F. Boccardi and H. Huang, “Zero-forcing precoding for the MIMO broadcast channel under per-antenna power constraints,” in *Proc. IEEE Signal Processing Advances in Wireless Commun. (SPAWC)*, 2006.
- [23] 3GPP TSG RAN and TR 25.814 v7.1.0, “Physical layer aspects for evolved UTRA,” Sept. 2006.
- [24] A. G. Burr, “Capacity bounds and estimates for the finite scatterers MIMO wireless channel,” *IEEE J. Select. Areas Commun.*, vol. 21, pp. 812–818, 2003.
- [25] ITU-R M.2134, “Requirements related to technical performance for IMT-advanced radio interface(s),” Dec. 2008.
- [26] B. Clerckx, G. Kim, and S. Kim, “Correlated fading in broadcast MIMO channels: Curse or blessing?” in *Proc. IEEE Glob. Telecom. Conf. (GLOBECOM)*, 2008.
- [27] W. Jakes and D. Cox, *Microwave mobile communications*. Wiley-IEEE Press, 1994.
- [28] D. Hammarwall, M. Bengtsson, and B. Ottersten, “Acquiring partial CSI for spatially selective transmission by instantaneous channel norm feedback,” *IEEE Trans. Signal Processing*, vol. 56, pp. 1188–1204, Mar. 2008.
- [29] A. S. Krishnamoorthy and M. Parthasarathy, “A multivariate gamma-type distribution,” *The Annals of Mathematical Statistics*, vol. 22, pp. 549–557, 1951.
- [30] I. Gradshteyn and I. Ryzhik, *Tables of Integrals, Series and Products*, 6th ed. San Diego CA: Academic, 2000.

TABLE I
COMPARISON OF FEEDBACK OVERHEAD AND CODEBOOK SIZE

Schedulers	Feedback overhead given B	Codebook size given B_u and B_t
GUS & SUS	M^2KB	$\min(\frac{B_u}{M}, \frac{B_t}{KM^2})$
NUS	MLB	$\min(\frac{B_u}{M}, \frac{B_t}{ML})$
LocalNUS	$(MK + ML)B$	$\min(\frac{B_u}{M}, \frac{B_t}{MK+ML})$
LUS	MLB	$\min(\frac{B_u}{M}, \frac{B_t}{ML})$

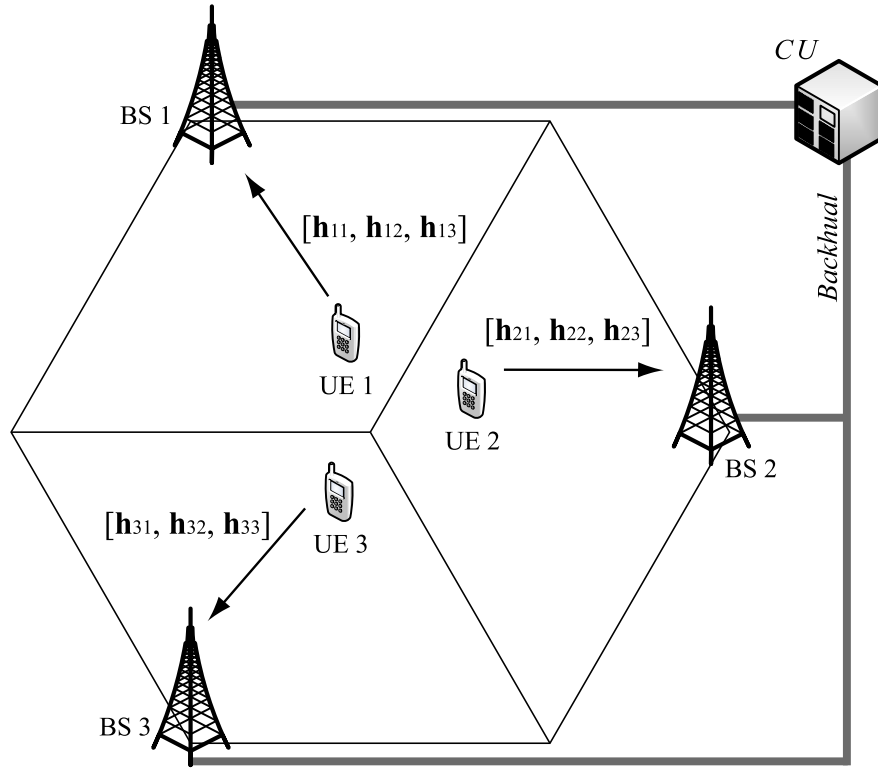


Fig. 1. Network layout of centralized CoMP systems.

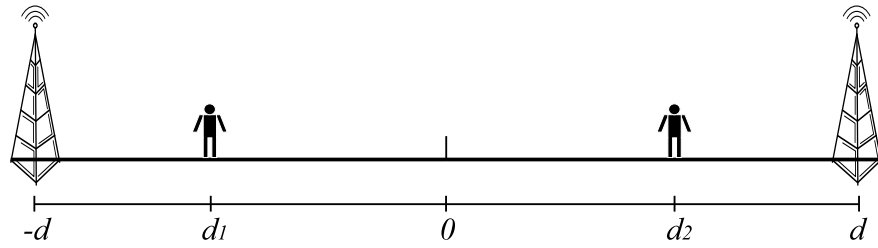


Fig. 2. The considered two-cell CoMP system for numerical analysis.

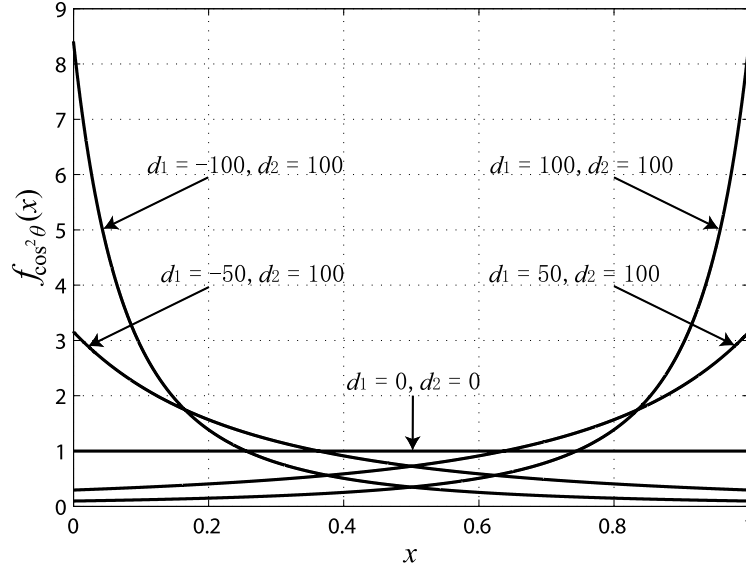


Fig. 3. The pdf of $\cos^2 \theta$ with respect to different user locations.

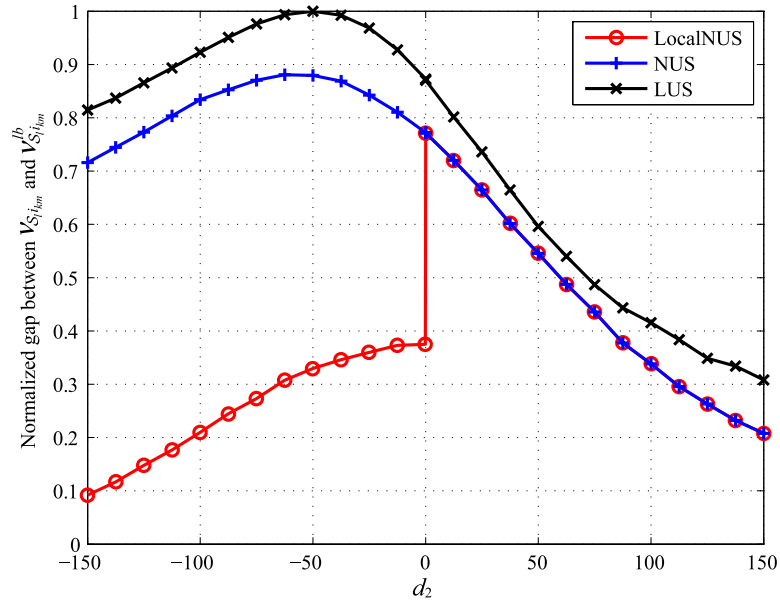


Fig. 4. Normalized gap between $\nu_{S_{l i_{km}}}$ and $\nu_{S_{l i_{km}}}^{lb}$ with respect to the position of user i_{km} . To simplify the notation, here we use $\nu_{S_{l i_{km}}}^{lb}$ to denote the lower bounds of $\nu_{S_{l i_{km}}}$ for the NUS, the LocalNUS and the LUS. The results are averaged over 10000 small-scale Rayleigh fading channels consisting of independent and identically distributed (i.i.d.) complex Gaussian variables with zero mean and unit variance.

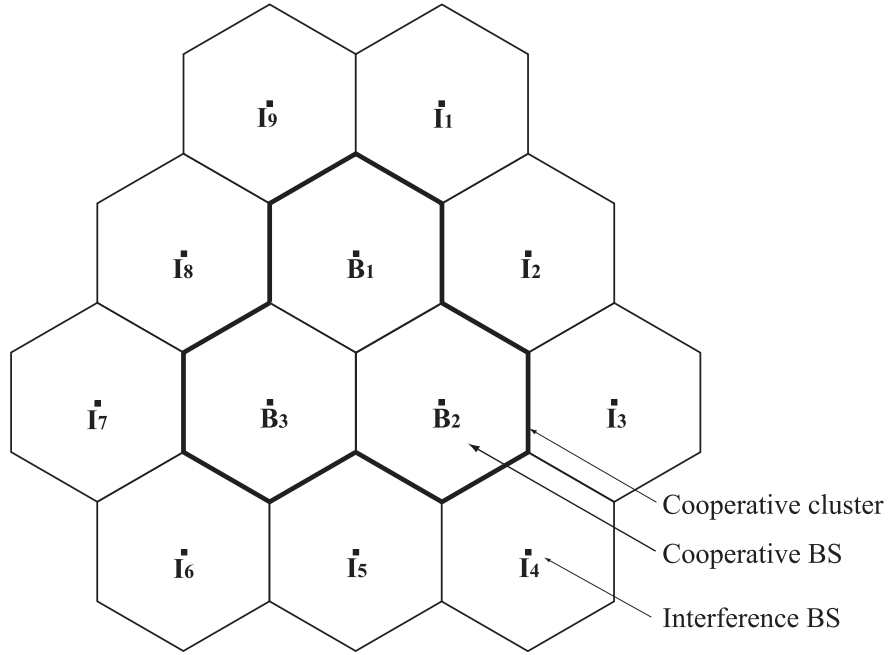


Fig. 5. Network layout for simulation: a cooperative cluster consisting of 3 coordinated BSs surrounded by 9 interfering cells.

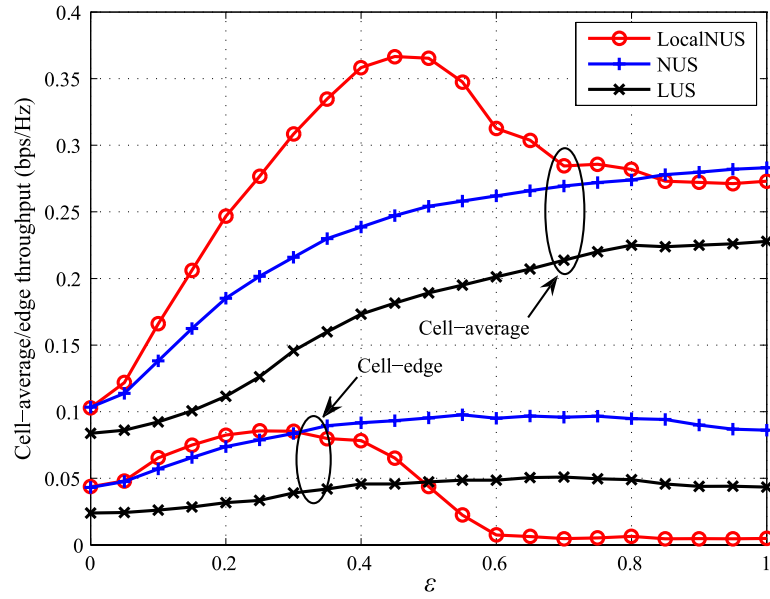


Fig. 6. Cell-average and cell-edge throughput of the NUS, the LocalNUS and the LUS as a function of ϵ with perfect CSI for precoding.

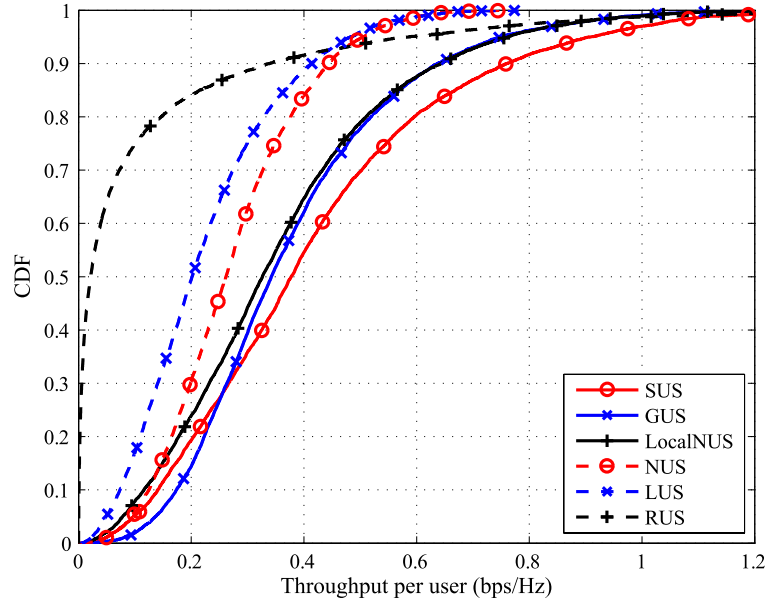


Fig. 7. The CDF of the throughput achieved by each individual user assuming perfect CSI for precoding. The thresholds for the SUS, the LocalNUS, the NUS, and the LUS are chosen as 0.5, 0.4, 0.8 and 0.8, respectively, which are also used in Fig. 8, Fig. 9, Fig. 10 and Fig. 11.

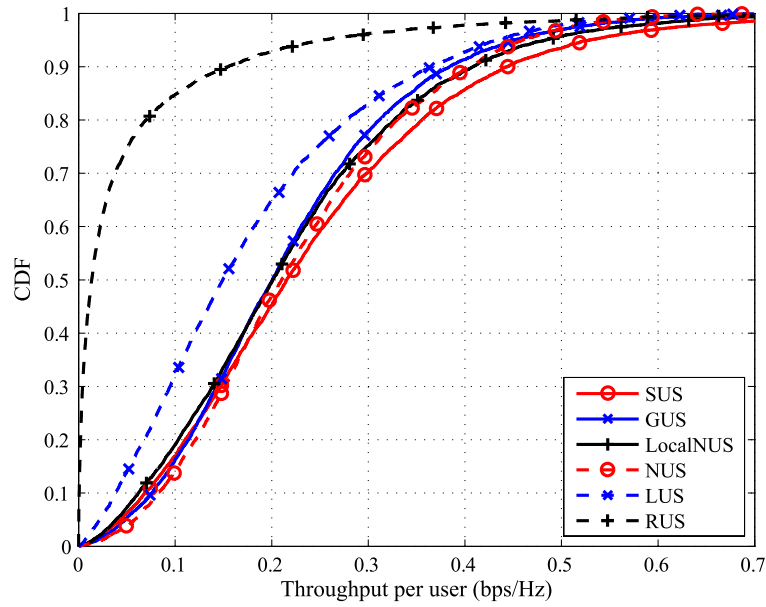


Fig. 8. The CDF of the throughput achieved by each individual user considering limited feedback. The angular spread is set to be 15 degrees.

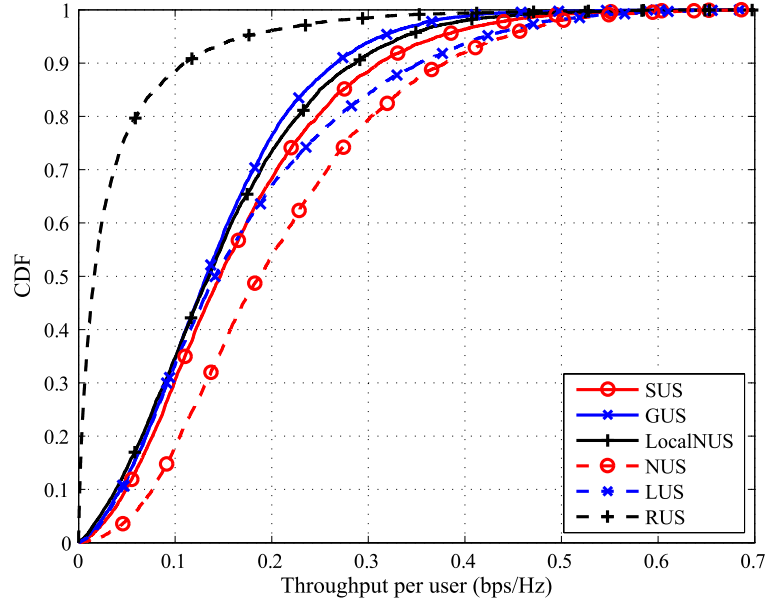


Fig. 9. The CDF of the throughput achieved by each individual user considering limited feedback. The angular spread is set to be 35 degrees.

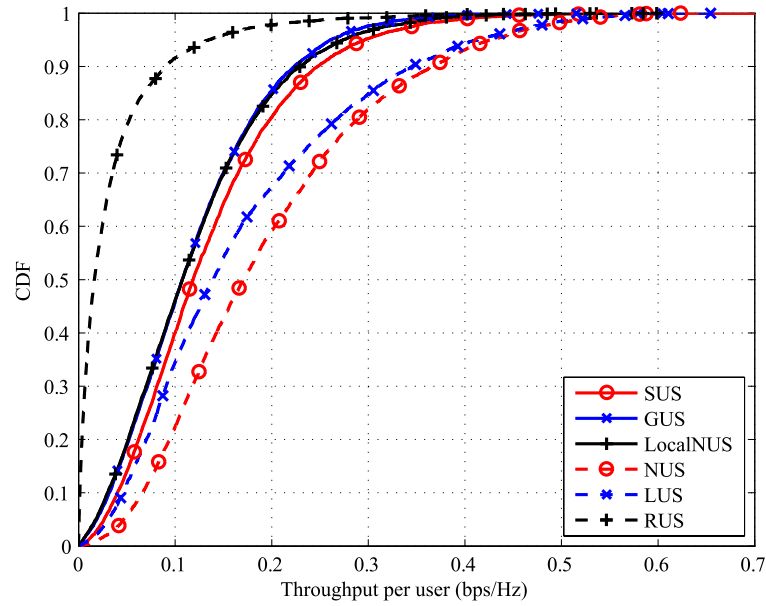


Fig. 10. The CDF of the throughput achieved by each individual user considering limited feedback. The angular spread is set to be 360 degrees.

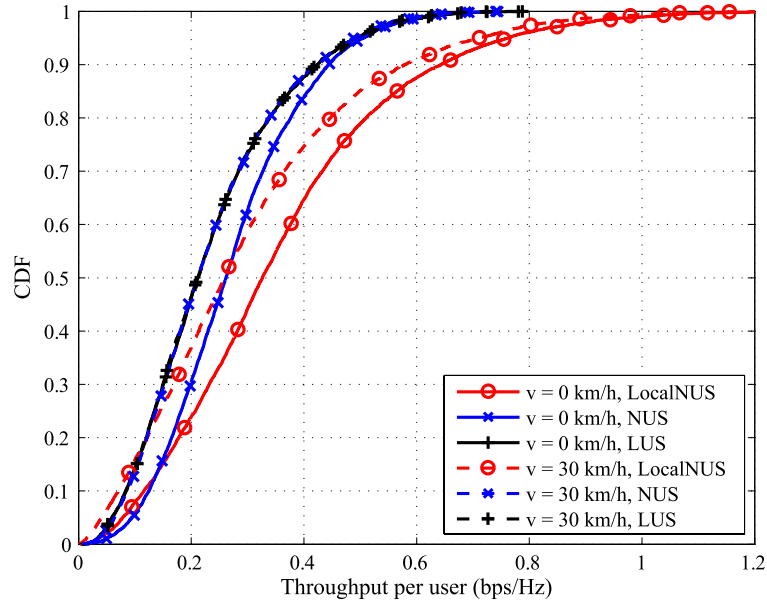


Fig. 11. The CDF of the throughput achieved by each individual user in time-varying channels. The operation frequency is 2 GHz. The results of the LUS for $v = 0$ km/h and $v = 30$ km/h overlap with the result of the NUS for $v = 30$ km/h.